

MISCELLANEOUS

MEASUREMENT OF THE ABLATION OF HEAT SHIELD MATERIALS BY FIBER-OPTICAL SENSORS

G. F. Gornostaev, V. V. Pasichnyi,  
and G. V. Tkachenko

UDC 536.3:681.586.5

*The results of the elaboration, testing, and application (in bench studies) of fiber sensors of linear ablation of a heat shield material are presented. The measuring technique and the structural arrangement of the sensors designed for products of the research and production association (RPA) "Energiya" and the design office "Novator" (Russia) have been described. Methods for manufacturing a ceramic tip equipped with fiber ablation sensors have been developed.*

To obtain experimental data on changes in the thickness of the heat-resistant coating of the frontal parts of spacecraft as they enter into dense atmospheres, they are equipped with heat shield ablation sensors. Such devices are also used in the bench development of new heat shield materials.

Of the existing types of mass ablation sensors (MAS) — fiber, radiotechnical, ultrasonic sensors, radiotracers, thermoelectric, electric, electromechanical sensors — the most universal and high-precision devices are the fiber ones [1].

Fused silica fibers of diameter 1 mm were pasted in holes of diameter 1.1 mm (Fig. 1). A photographic head with SFZ-1 cadmium selenide photoresistors was fastened to the specimen on the underside on centering pins. Thermostabilization of the photodetectors is carried out by means of lithium nitrate trihydrate  $\text{LiNO}_3 \cdot 3\text{H}_2\text{O}$  having a melting point of  $30^\circ\text{C}$  and a specific melting heat  $r = 2.9 \cdot 10^5$  J/kg. Thermostabilization aids in retaining the intrinsic noise level and time constants, which depend on the temperature of the sensitive layer of the photodetector. Such a design of the MAS was developed to the order of the RPA "Energiya" (Russia) for "Mars-5."

In high-temperature materials based on asbestos-filled plastics (ASD), glass-reinforced plastic (STKT-11, TZMKT-8, STKT-NA) and carbon-filled plastic UP-UT-P, quartz optical fibers were set, and in low-sublimation materials based on polymers (TP-41K) and sawdust (TTPS-15), glass fibers were set. In each specimen, four optical fibers were set at a different distance from the heated surface of the material.

**Development of the Measuring Technique.** To determine the moment the upper end of the optical fiber appears on the destructed surface of the heat shield material HShM (STKT-11, ASD, TP-41, TTPS-15), a special study has been made. For each type of material, two optical fibers were set: one through fiber and one "internal" fiber whose input end was situated at a known distance  $h$  from the heated surface of the heat shield material. The results of testing such sensors on a gas-dynamic bench indicate that irrespective of the heating conditions ( $q = 0.67\text{--}1.76 \cdot 10^4$  kW/m<sup>2</sup>) the character of change in the luminous fluxes at the output of the above optical fibers was identical. The luminous flux from the "internal" fiber increases smoothly and reaches the level of the flux from the through fiber, and then stabilizes at this level:

$$J_{\text{thr.f}} - J_{\text{in.f}} \rightarrow 0, \quad \text{if } h \rightarrow 0.$$

---

I. N. Frantsevich Institute for Problems of Material Science, National Academy of Sciences of Ukraine, 3 Krzhizhanovskii Str., Kiev, 03142, Ukraine; email: pasich@ipms.kiev.ua. Translated from *Inzhenerno-Fizicheskii Zhurnal*, Vol. 81, No. 4, pp. 744–749, July–August, 2008. Original article submitted March 19, 2007; revision submitted October 9, 2007.

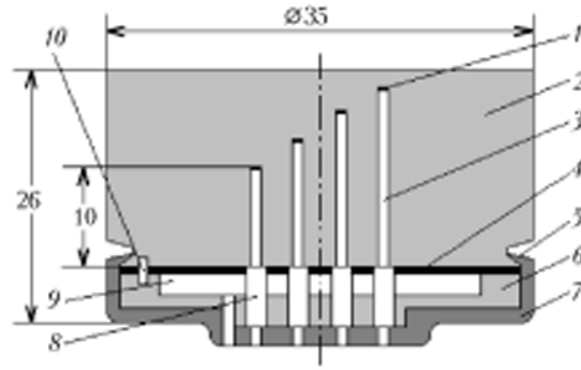


Fig. 1. Structural arrangement of the MAS: 1) rhodium film on the fiber end; 2) HShM TTPS-15; 3) fiber; 4) cover; 5) place of flaring; 6) cloth-based laminate bush; 7) metal case; 8) photodetector; 9) cavity with  $\text{LiNO}_3 \cdot 3\text{H}_2\text{O}$ ; 10) centering pin.

TABLE 1. Measurement Data for  $R_{op}$  of Sensors with through Optical Fibers Obtained on Convective and Radiant (SGU-4, "Uran") Heating Benches

Bench	Heating conditions			Heat shield material	$R_{op}$ , $k\Omega$	Fiber material and length L
	$q \cdot 10^{-4}$ , $\text{kW}/\text{m}^2$	$P_d \cdot 10^{-5}$ , Pa	$T_d$ , K			
Gas generator	0.09	1.05	1100	TTPS-15	16.0	Glass, $L = 40$ mm
	0.12	1.06	1200		6.5	
	0.33	1.1	1500		4.0	
SGU-4	0.92	—	—	TTPS-15	1.3	Glass, $L = 40$ mm
Gas generator	0.09	1.05	1100	TP-41K	14.0	Glass, $L = 40$ mm
	0.12	1.06	1200		6.0	
	0.33	1.1	1500		3.3	
"Uran"	0.5	—	—	TP-41K	2.0	Glass, $L = 40$ mm
	0.6	—	—		1.0	
	0.7	—	—		0.5	
Gas generator	0.55	1.3	1800	ASD	2.6	Quartz, $L = 40$ mm
	1.0	1.9	2500		1.0	
	1.76	3.5	3100		0.70	
Gas generator	0.55	1.3	1800	STKT-11	—	Quartz, $L = 40$ mm
	1.0	1.9	2500		—	
	1.76	3.5	3100		—	
"Uran"	0.63	—	—	STKT-11	0.35	Quartz, $L = 40$ mm
Gas generator	4.2	110	3100	Niasit	0.70	Quartz, $L = 190$ mm

Thus, the value of the photoresistance  $R_{op}$  corresponding to the moment the "internal" fiber end appears on the destroyed surface of the HShM can be estimated from the value of the photoresistor situated under the through fiber (Table 1). This fact considerably reduced the duration of the bench experiment on the determination of the  $R_{op}$  value for various classes of HShMs and their heating conditions.

Taking into account that the stabilization moment of the internal fiber signal corresponds to the moment its upper end appears on the destroyed surface of the material, we have plotted ablation graphs for different HShMs from the readings of the photodetectors. The fibers have no influence on the destruction of the HShM surface.

**Error Analysis.** To avoid the influence of the outer radiation flux penetrating through the semitransparent layer of the HShM on the ablation measurement accuracy, the input ends and part of the lateral surface of the fiber are covered with a light-tight film of rhodium having high reflective and mechanical properties and a high thermostability. Upon annealing in argon at a temperature of  $\sim 970$  K the Rh film is compacted to a thickness of 4–7  $\mu\text{m}$ . The data of pet-

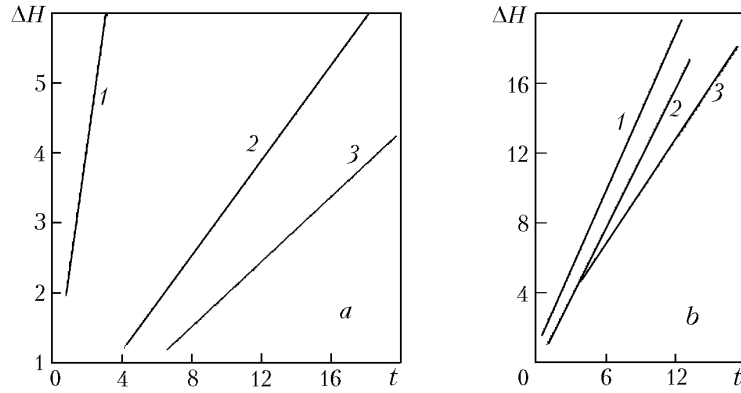


Fig. 2. Data on the ablation of high-temperature (a) and low-sublimating (b) HShMs obtained on different hydrodynamic benches by means of fiber-optical sensors: a) KT-8,  $q = 2.7 \cdot 10^4$  kW/m<sup>2</sup>,  $P_d = 1.8$  MPa,  $T_d = 5500$  K; 2) ASD,  $q = 0.76 \cdot 10^4$  kW/m<sup>2</sup>,  $P_d = 1.7 \cdot 10^5$  MPa,  $T_d = 2300$  K; 3) UP-TK-P,  $q = 1.2 \cdot 10^4$  kW/m<sup>2</sup>,  $P_d = 2.3 \cdot 10^5$  MPa,  $T_d = 2600$  K; b) 1) TP-41K,  $q = 0.33 \cdot 10^4$  kW/m<sup>2</sup>,  $P_d = 1.1 \cdot 10^5$  MPa,  $T_d = 1500$  K; 2) TTPS-15,  $q = 0.33 \cdot 10^4$  kW/m<sup>2</sup>,  $P_d = 1.1 \cdot 10^5$  MPa,  $T_d = 1500$  K; 3) fluoroplastic-4,  $q = 1.2 \cdot 10^4$  kW/m<sup>2</sup>,  $P_d = 2.3 \cdot 10^5$  MPa,  $T_d = 2600$  K.  $\Delta H$ , mm;  $t$ , sec.

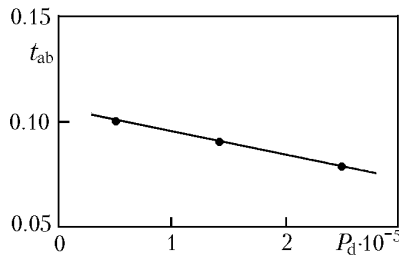


Fig. 3. Ablation time of the rhodium film on the fiber end versus the stagnation pressure of the gas generator jet (STKT-11).  $t_{ab}$ , sec;  $P_d$ , Pa.

rographic analysis of glass and quartz optical fibers after their operation in the HShM (TTPS-15, TP-41K, ASD, STKT-11) point to the absence of interaction between the rhodium film and the fibers. Fusion of rhodium has not been observed either.

To estimate the destruction (ablation) time of the rhodium film, we have tested sensors with through light-tight optical fibers on a gas-dynamic bench. The time  $t_{ab}$  after which the recording threshold trigger unit — the sensor signal transformer (PSD-10) — operated was registered. The test data (Fig. 3) indicate that the PSD-10 operated at the threshold value of the photoresistance  $R_{op}$  corresponding to a given heat flux in a time not exceeding 0.1 sec after the beginning of heating. The source of the light signal was the outer radiation which acted on the photodetector upon ablation of the rhodium film.

The operative reliability of the sensors was estimated by the number of nonsequential ("false") operations of individual sensors with respect to their total number (20 operations for each HShM). At a sealing "pitch" of the fiber ends equal to 1.0 mm operation of discrete individual sensors occurred sequentially practically in all tested specimens, i.e., in the order in which the fiber ends were positioned relative to the heated HShM surface. The high reliability of the operation of the MASs with a "stopper" with sensors pasted in the hole on the heat shield has been confirmed by testing sensors from the HShMs TP-41K and TTPS-15 in jets of two gas generators with the following parameters: 1)  $q = 0.3 \cdot 10^4$  kW/m<sup>2</sup>,  $P_d = 2 \cdot 10^5$  Pa,  $T_d = 6800$  K; 2)  $q = 0.16 \cdot 10^4$  kW/m<sup>2</sup>,  $P_d = 0.4 \cdot 10^5$  Pa,  $T_d = 3000$  K.

The fluctuation of the light signal at the output from the through fiber introduces uncertainty into the choice of the  $R_{op}$  value. At a value of  $R_{op}$  equal to the mean value of  $R_{phd}[J_{thr.f}(h = 0)]$  the error  $\delta R_{op}$  is no more than  $\pm 3\%$

TABLE 2. Measurement Data for the HShM Ablation and Response Error of the Sensors Obtained on Gas-Dynamic Benches of Different Enterprises

Enterprise	Heating conditions			Heat shield material	$V_{ab}$ , mm/sec	$\Delta H$ , $\pm$ mm
	$q \cdot 10^{-4}$ , kW/m <sup>2</sup>	$P_d \cdot 10^{-5}$ , Pa	$T_d$ , K			
IPM NAS of Ukraine	0.33	1.1	1500	TP-41K	1.3	0.4
	0.33	1.1	1500	TTPS-15	1.1	0.4
	0.67	1.55	2200	ASD	0.32	0.5
	0.76	1.7	2300	ASD	0.36	0.5
	1.20	2.3	2600	UP-UT-P	0.2	0.8
	1.76	3.5	3100	ASD	0.48	0.5
RPA "Energiya" (Russia)	0.16	0.4	3000	TP-41K	0.5	0.4
	0.16	0.4	3000	TTPS-15	0.4	0.4
RIPI	2.7	18	5000	HShM KT-8	2.0	0.5
Votkin engineering plant (Russia)	4.2	110	3100	Niasit	0.98	0.5

( $q \leq 1.76 \cdot 10^4$  kW/m<sup>2</sup> (according to the results of experiments on the gas-dynamic bench) for the materials TP-41K, STKT-11, TTPS-15, and ASD.

The error due to the finite width of the change-of-state zone of the PSD-10 signal transformer operating at  $R_{phd} = R_{op}$  is about  $\pm 3\%$ . An important role in the question on the measurement error of linear ablation of the HShM by a discrete MAS is played by the sealing accuracy of the fiber ends at a given distance from the heated surface of the HShM. The error of X-ray control of the coordinates of the fiber ends covered with Rh film was  $\sim 0.4$  mm.

On the gas-dynamic bench of the Institute for Problems of Material Science (IPM), National Academy of Sciences of Ukraine, the error of a discrete MAS was determined as follows. As soon as the unit of the PSD-10 operated, its output signal (6 V) actuated, through a relay, a double-action pressure-operated electric valve, which controls the system of introduction-removal of the sting from the jet. Upon removal of the specimen with a sensor from the jet, its linear measurement was made. The error  $\delta H$  in determining the thickness of the ablated HShM layer by a single sensor was estimated from the mean velocity  $V_{ab}$  of HShM ablation by comparing the initial  $L_{in}$  and final (after cessation of heating)  $L_{fin}$  of the fiber length:

$$\delta H = V_{ab} \Delta t_{iner} - (L_{in} - L_{fin}) . .$$

Table 2 presents the ablation measurement data and the error of the sensors.

#### Results of Measurements of the Heat Shield Ablation and Technology of Making a Tip with MASs.

Measurements of the HShM KT-8 ablation were taken on the gas-dynamic plant of the Research Institute of Precision Instruments (RIPI, Russia). Concurrent monitoring of the ablation value of the material was carried out by filming (1 frame per second). The testing conditions were as follows:

$$q = 2.7 \cdot 10^4 \text{ kW/m}^2, \quad P_d = 1.8 \text{ MPa}, \quad T_d = 5500 \text{ K} .$$

The results of the filming data processing indicate that quartz fibers and the HShM are ablated with an equal velocity, the fibers have no influence on the destruction of the heated surface, and the accuracy of measurements of the linear ablation of the material by the sensors is equal to  $\pm 0.5$  (Fig. 2a, Table 2).

On the gas-dynamic bench of the Votkin engineering plant (Russia), we obtained, with the use of sensors, data on the ablation of a ceramic tip under the following heating conditions [2]:  $P_d = 11$  MPa,  $T_d = 3100$  K,  $q = 4.2 \cdot 10^4$  kW/m<sup>2</sup>. The results of processing the data on the tip ablation obtained by means of eight discrete sensors are presented in Fig. 4, where the coordinates of the input ends of the fibers are schematically brought together in one plane and are positioned on one side on the cone axis. Alongside the coordinate, the response time of the corresponding sensor is given.

The filming data point to the fact that the accuracy of measuring the linear ablation by the sensors was  $\pm 0.5$  mm (Table 2). The quartz fibers have no influence on the destruction of the material (niasit) in the places where sen-

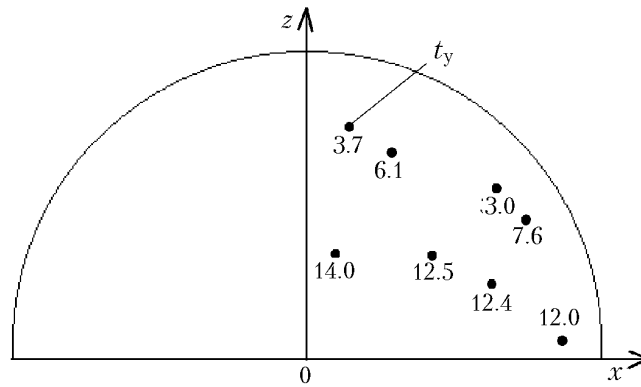


Fig. 4. Position of fiber ends covered with rhodium film and response time of the corresponding sensor, sec.

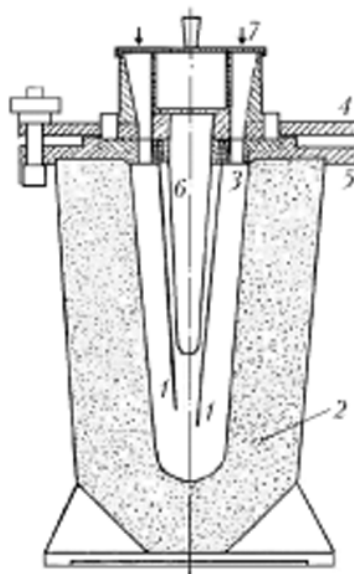


Fig. 5. Molding set for slip casting of tips with fibers: 1) fibers; 2) gypsum mold; 3) guide bushes; 4, 5) upper and lower flanges, respectively; 6) metal finger; 7) liquid slip feed.

sors are located. The measurement data for the HShM ablation on the gas-dynamic benches of the IPM, NAS of the Ukraine, are presented in Fig. 2 and in Table 2.

Products of the design office "Novator" (Russia) use quartz tips from Niasit of the following design: the cone height is 190 mm, the dulling radius of the point nose is 20 mm.

We have developed a design and methods for making a tip from quartz ceramics rigged with fiber-optical MASs in the process of heat shield formation. The technological process of making a tip together with quartz fibers (of diameter 1–1.2 mm) includes the following operations: preparation of glass and slip; making and preparation of gypsum molds; molding; drying and annealing; mechanical treatment; assembly; application of a moisture-proof coating.

The tip with fibers represents a cone, inside of which 10 fibers of length 170–185 mm and an adjusting fiber of length 15 mm are positioned. On the end of the product OTI-2252, the fibers are arranged in a circle at an equal distance from one another. In the vertex of the cone, all fibers are situated at a different height and at a different distance from the tip surface where the position of the rhodium-film-covered fiber is determined by the length of the fiber and the angle of inclination to the cone axis. The general view of the molding set for forming a tip is given in Fig. 5. To prepare a slip, we use quartz glass TU 1.702.001-78 and rods from transparent quartz glass which are used to make milling bodies. The slip is prepared in a mill. To make the blank, the slip is deposited on the gypsum surface

of the mold completely following the outer surface of the blank. The slip-filled molds are left for 10–16 h, then the mold for the tip is stripped, and the blank is dried (for 1.5–2 h), shrinks a little, and easily goes out of the mold. Drying and annealing of blanks includes: airing-off at room temperature for 1–2 days; annealing in an electric furnace (heating to a temperature of  $1520 \pm 30$  K and cooling to 570 K); working of the ends and outer surface of the tip blanks on a lathing-screw-cutting machine until the tip attains the final dimensions.

According to the technological process and technological conditions, in each batch (5 pieces) of products, the bending strength (51–65 MPa) and the density ( $1.91\text{--}2.00$  g/cm<sup>3</sup>) were determined. The bending strength values for the reinforced (65 MPa) and nonreinforced (67 MPa) ceramics are nearly equal.

As the results of mechanical tests have shown, the impact strength of the products increases by about a factor of 1.6 as the number of fibers in the cross-section of the specimen is changed from 0 to 5 pieces. The value of the elasticity modulus ( $3580\text{--}3730$  kg/mm<sup>2</sup>) remains at the level of the nonreinforced ceramics.

Bearing capacity tests for the tip with fibers were conducted in accordance with the scheme of loading a real tip. Loading was carried out by smoothly increasing the force  $F$  from 0 to 4400 N and further to destruction of the product. For three specimens destruction occurred in the section coinciding with the embedment depth of the "finger" at loads of 5490–7350 N. The safety factor of the product with sensors is in the 1.22–1.66 range, which corresponds to the safety factor for the full-scale tip. The dielectric properties of the fiber-reinforced quartz ceramics were determined on the setup "Kvartz," and at room temperature they were as follows: dielectric constant 3.34–3.39 and dielectric loss tangent  $\leq 5$ , which corresponds to the values of these parameters for the nonreinforced ceramics. As the temperature is increased to 1473 K, the value of the dielectric constant increases to 3.54, and the dielectric loss tangent increases to 105. The X-ray results point to the absence of structural defects in the tip material and to its solidity.

The bush with photodetectors is solidly set on a metal "finger." The SFZ-1 soldered connections on the screened electric cable situated inside the "finger" are insulated and encapsulated with epoxy resin. To protect the sensitive surface of the photodetector from the outer radiation penetrating through the ceramics, the lower end surface of the tip around the fibers was blanckened with graphite. The measurement data for the ablation of such a tip are given above.

## CONCLUSIONS

1. We have developed a design of a discrete MAS for semitransparent HShMs, which operates independent of the optical properties of HShMs and the presence of chemically active carbon in the coke layer of the material. The relatively low heat conduction of the fibers makes the heat flows through the sensor into the depth of the material insignificant. The accuracy of controlling the ablation of high-temperature HShMs by the optoelectronic MAS (Table 2) exceeds the accuracy of the ultrasonic ( $\pm 1.27$  mm) and radioactive ( $\pm 2.8$  mm) sensors; in carbon-filled plastic its accuracy ( $\pm 0.8$  mm) exceeds the accuracy of the thermocouple sensor ( $\pm 1.5$  mm), and in glass-reinforced plastic it gives a twice smaller error ( $\pm 0.5$  mm) than the radiotechnical MAS ( $\pm 1.0$  mm). In a sublimating HShM, the optoelectronic MAS permits ablation control with an accuracy of  $\pm 0.4$  mm and practically has no rivals. Overall, the above features of the optoelectronic MASs make them preferable in investigating quartz ceramics, sublimating HShMs, asbestos-filled plastic, glass-reinforced plastic, and, likely, carbon-filled plastic.

2. For the first time a working means for controlling the ablation of the quartz ceramic tip, which practically ideally blends with the product material, has been developed. The technology of making a tip with MASs makes it possible to preserve the basic properties (structure, integrity, strength, radiopacity, density) of the product and increase its impact strength. The output signal of the ablation sensor is easily matched to the measuring system on board a space vehicle. The technological process of making a tip with MASs was brought to a commercial level at the pilot production department of the research and production association "Tekhnologiya" (Russia); the tips were recognized as suitable for furnishing the product 63T6 of the design office "Novator" (Russia).

3. The results of bench tests of discrete MASs under convective heating at the enterprises the IPM, NAS of Ukraine, the Votkin engineering plant (Russia), the RIPI (Russia), and the RPA "Energiya" (Russia) indicate that the sensors make it possible to measure the ablation of a wide class of heat shield materials and have no appreciable influence on the destruction of the investigated HShMs. As a result of using the sensors in the bench tests, data on the ablation velocity of different classes of heat shield materials have been obtained.

## NOTATION

$F$ , force, N;  $h$ , distance from the upper end of the "internal" optical fiber to the heated surface of the HShM, mm;  $J_{in.f}$ , light flux at the output of the "internal" fiber, W;  $J_{thr.f}$ , light flux at the output of the through fiber, W;  $L_{in}$  and  $L_{fin}$ , initial and final lengths of the fiber, respectively, mm;  $P_d$ , stagnation pressure of the gas jet, Pa;  $q$ , heat flux density on the HShM surface, kW/m<sup>2</sup>;  $r$ , specific melting heat, J/kg;  $R_{op}$ , value of the photodetector resistance, at which operation of the sensor occurs, k $\Omega$ ;  $R_{phd}$ , value of the photodetector resistance, k $\Omega$ ;  $t$ , time of the experiment, sec;  $t_{ab}$ , rhodium film ablation time, sec;  $T_d$ , stagnation temperature of the gas jet, K;  $V_{ab}$ , HShM ablation velocity, mm/sec;  $x$ , tip radius, mm;  $z$ , tip axis;  $\Delta H$ , value of the linear ablation of the HShM, mm;  $\Delta t_{iner}$ , inertia of the input–output system of the holder, sec;  $\delta H$ , error in determining the value of the linear ablation, mm;  $\delta R_{op}$ , error in determining the value of  $R_{op}$ ; %. Subscripts: in.f, "internal" fiber; iner, inertia; fin, final; in, initial; op, operation; thr.f, through fiber; phd, photodetector; ab, ablation; d, stagnation.

## REFERENCES

1. G. F. Gornostaev, Fiber-optical sensors and prospects of using them in the space program of Ukraine, *Kosm. Nauka Tekhnol.*, No. 3-4, 88–94 (1996).
2. G. F. Gornostaev, V. V. Pasichnyi, and G. V. Tkachenko, Method of measuring the radiant component of a heat flux on the surface of ceramic heat shields material, *Kosm. Nauka Tekhnol.*, No. 2-3, 98–102 (2006).